Available online at www.sciencedirect.com
SCIENCE DIRECT®
Inorganica Chimica Acta 357 (2004) 809–816
Inorganica Chimica Acta
www.elsevier.com/locate/ica

Spectroscopic and structural characterizations of ammonium peroxo–carboxylato molybdate(VI) complexes

D. Bayot [a], B. Tinant [b], M. Devillers [a,*]

[a] Unité de Chimie des Matériaux Inorganiques et Organiques, Université Catholique de Louvain, Place Louis Pasteur 1/3, B-1348 Louvain-la-Neuve, Belgium
[b] Unité de Chimie Structurale et des Mécanismes Réactionnels, Université Catholique de Louvain, Place Louis Pasteur 1/3, B-1348 Louvain-la-Neuve, Belgium

Received 11 June 2003; accepted 20 September 2003

Abstract

New ammonium derivatives of peroxo–carboxylato molybdenum(VI) complexes of general formula $(NH_4)_2[MoO(O_2)_2(H_xL)]\cdot nH_2O$ with L = oxalate (ox), citrate (cit), tartrate (tart), glycolate (glyc) and malate (mal) and $(NH_4)_2[MoO_2(O_2)(L)]$ with L = oxalate (ox) have been prepared and characterized on the basis of elemental and thermal analysis as well as by IR and ^{13}C NMR spectroscopy. These last two spectroscopic methods have been used to suggest the coordination mode of the ligand in the complexes. The X-ray crystal structures of the compounds $(NH_4)_2[Mo_2O_2(O_2)_2(OH)_2(ox)_2]$, $(NH_4)_2[MoO(O_2)_2(ox)]$ and $(NH_4)_2[MoO(O_2)_2(glyc)]\cdot 0.5EtOH$ have been determined, all showing a sevenfold-coordinated Mo atom with bidentate peroxides and carboxylate ligands.

Keywords: Peroxo-carboxylato molybdenum(VI) complexes; Crystal structures; IR spectra; ^{13}C NMR

1. Introduction

In the last decade, peroxo and peroxo–carboxylato compounds of transition metals have attracted considerable attention because many of them are efficient stoichiometric or catalytic oxidants for organic compounds [1,2]. According to many studies [3,4], carboxylato anions capable of forming a five-membered chelate ring with the metal atom are very suitable ligands for peroxo-complexes of Mo, W, Nb or Ta. As far as peroxo molybdenum(VI) compounds are concerned, the studies carried out up to now essentially concerned mononuclear complexes of general formula $K_2[MoO(O_2)_2(H_xL)]\cdot nH_2O$ (L = oxalate, citrate, tartarte, tartronate, quinolate, malate and glycolate) [4–7], $K_2[MoO_2(O_2)(L)]$ (L = oxalate) [4] in which the ligand is always bidentate and dinuclear complexes like $K_4[Mo_2O_2(O_2)_4(L)]\cdot 4H_2O$ (L = tartrate) in which the ligand is a tetradentate bridging tartrate [4,8]. Complementary research on these compounds is driven by their potential use as molecular precursors for the preparation of Mo-based oxide-type materials, because the presence of alkaline metal ions like potassium leads to contamination of the final solid materials and is consequently a severe drawback. The preparation of similar compounds with non-metallic counter-ions that would leave no residue upon thermal degradation under appropriate conditions is therefore particularly welcome.

The present work is dedicated to new peroxo–carboxylato Mo(VI) compounds containing ammonium as counter-ion, corresponding to the general formula $(NH_4)_2[MoO(O_2)_2(H_xL)]\cdot nH_2O$ with L = oxalate (ox), citrate (cit), tartrate (tart), glycolate (glyc) and malate (mal), and $(NH_4)_2[MoO_2(O_2)(L)]$ with L = oxalate (ox). This paper reports the synthesis and the structural and spectroscopic characterization of these compounds. In the meantime, when associated

* Corresponding author. Tel.: +32-10-472-827/831; fax: +32-10-472-330.
E-mail address: devillers@chim.ucl.ac.be (M. Devillers).

0020-1693/$ - see front matter © 2003 Elsevier B.V. All rights reserved.
doi:10.1016/j.ica.2003.09.012

with analogous compounds containing niobium, the compounds described here have been successfully used for the preparation of Nb–Mo oxides supported on silica [9].

2. Experimental

2.1. General procedures

The syntheses of the ammonium peroxo–carboxylato molybdenum compounds were adapted from the procedures used by Dengel et al. [4] to obtain the similar potassium derivatives.

All reagents, oxalic acid dihydrate, $H_2ox \cdot 2H_2O$ (Merck), ammonium oxalate monohydrate, $(NH_4)_2ox \cdot H_2O$ (Merck), citric acid monohydrate, $H_4cit \cdot H_2O$ (Merck), DL-tartaric acid, H_4tart (Acros Organics), DL-malic acid, H_3mal (Alfa Aesar), glycolic acid, H_2glyc (Acros Organics) and ammonium heptamolybdate tetrahydrate (AHM), $(NH_4)_6Mo_7O_{24} \cdot 4H_2O$ (Acros Organics) were commercial products used as received. Hydrogen peroxide H_2O_2 (35 wt%, Acros), ammonium hydroxide NH_4OH (25 wt%), ethanol and acetone were used without purification.

Elemental analyses (C, H, N) were carried out at the University College of London. IR spectra in the 4000–400 cm^{-1} range were recorded on a FTS-135 Bio-Rad spectrometer, using KBr pellets containing ca. 1 wt% of the powder. Thermogravimetric analyses (TGA) were performed in air at the heating rate of 10 °C/min using a Mettler Toledo TGA/SDTA851^e analyser. The ^{13}C NMR spectra were recorded at 125 MHz in D_2O on a Bruker Avance 500 MHz spectrometer.

2.2. Preparation of the complexes

2.2.1. Preparation of $(NH_4)_2[MoO_2(O_2)(ox)] \cdot H_2O$ (**Ia**)

AHM (0.74 g, 4.2 mmol Mo) was dissolved in a solution (20 ml) of $H_2ox \cdot 2H_2O$ (0.23 g, 1.8 mmol) and $(NH_4)_2ox \cdot H_2O$ (0.34 g, 2.4 mmol). The resulting clear solution was treated with a stoichiometric amount of a 35 wt% H_2O_2 solution (0.41 ml, 4.2 mmol). Addition of a few drops of ethanol and storage at 5 °C for a week yielded a yellow precipitate which was filtered off, washed with ethanol and air-dried. Yield: 0.21 g, 16%. *Anal.* Calc. for $C_2H_{10}MoN_2O_9$: C, 7.95; H, 3.31; N, 9.27. Found: C, 8.34; H, 3.29; N, 9.49%. The slow evaporation at room temperature of an aqueous concentrated solution yielded after several weeks bright-yellow triangular crystals **Ib**, corresponding to the stoichiometry $(NH_4)_2[Mo_2O_2(O_2)_2(OH)_2(ox)_2]$. We also observed in the crystallization vessel small needle-like white crystals, probably corresponding to excess oxalic acid.

2.2.2. Preparation of $(NH_4)_2[MoO(O_2)_2(ox)]$ (**II**)

AHM (0.74 g, 4.2 mmol Mo) was dissolved in a solution (20 ml) of $H_2ox \cdot 2H_2O$ (0.23 g, 1.8 mmol) and $(NH_4)_2ox \cdot H_2O$ (0.34 g, 2.4 mmol). The resulting clear solution was treated with an excess of a 35 wt% H_2O_2 solution (10 ml) and became dark yellow. After 2 h stirring, addition of ethanol (100 ml) precipitated a yellow crystalline solid which was filtered off, washed with ethanol and air-dried. Yield: 1.06 g, 84%. *Anal.* Calc. for $C_2H_8MoN_2O_9$: C, 8.00; H, 2.66; N, 9.33. Found: C, 8.06; H, 2.27; N, 9.26%. The slow evaporation at room temperature of an aqueous concentrated solution yielded after several days long acicular yellow crystals of compound **II**.

2.2.3. Preparation of $(NH_4)_2[MoO(O_2)_2(H_2cit)]$ (**III**)

AHM (5 g, 28.3 mmol Mo) and $H_4cit \cdot H_2O$ (5.95 g, 28.3 mmol) were dissolved in 25 ml of distilled water. The resulting clear solution was treated with a 35 wt% H_2O_2 solution (10 ml) and ammonia (3 ml). After 2 h stirring, the solution was evaporated up to a final volume of ca. 10 ml. Addition of acetone (20 ml) yielded a yellow highly hygroscopic solid which was filtered off under nitrogen, then washed with acetone and dried under vacuum. Yield: 4.32 g, 38%. *Anal.* Calc. for $C_6H_{14}MoN_2O_{12}$: C, 17.91; H, 3.48; N, 6.97. Found: C, 17.77; H, 3.51; N, 6.79%.

2.2.4. Preparation of $(NH_4)_2[MoO(O_2)_2(H_2tart)] \cdot 2H_2O$ (**IV**)

AHM (1 g, 5.66 mmol Mo) and DL-H_4tart (0.85 g, 5.66 mmol) were dissolved in 25 ml of distilled water. The solution was treated with a 35 wt% H_2O_2 solution (10 ml) and ammonia (1 ml). After 2 h stirring, ethanol (50 ml) was added. After standing 24 h at room temperature, a yellow crystalline solid appeared and was filtered off, washed with ethanol and air-dried. Yield: 1.54 g, 69%. *Anal.* Calc. for $C_4H_{16}MoN_2O_{13}$: C, 12.12; H, 4.04; N, 7.07. Found: C, 11.81; H, 3.75; N, 6.90%.

2.2.5. Preparation of $(NH_4)_2[MoO(O_2)_2(glyc)]$ (**Va**)

AHM (2.5 g, 14.1 mmol Mo) and H_2glyc (1.08 g, 14.1 mmol) were dissolved in 25 ml of distilled water. The solution was treated with a 35 wt% H_2O_2 solution (10 ml) and ammonia (3 ml) and then evaporated up to a final volume of ca. 10 ml. Addition of ethanol (50 ml) and storage at 5 °C for one week yielded needle-like hygroscopic yellow crystals which were filtered off and air-dried. Yield: 2.79 g, 69%. *Anal.* Calc. for $C_2H_{10}MoN_2O_8$: C, 8.39; H, 3.10; N, 9.79. Found: C, 8.29; H, 3.60; N, 9.60%. Some of these crystals **Vb** were kept in solution waiting for X-ray analysis and corresponded to the stoichiometry $(NH_4)_2[MoO(O_2)_2(glyc)] \cdot 0.5EtOH$.

*2.2.6. Preparation of $(NH_4)_2[MoO(O_2)_2(Hmal)]\cdot H_2O$ (**VI**)*

A solution of DL-H_3mal (1.52 g, 11.33 mmol) in distilled water (10 ml) and ammonia (3 ml) was added to a clear solution of AHM (2 g, 11.33 mmol Mo). The resulting solution was treated with a 35 wt% H_2O_2 solution (10 ml) and then evaporated up to a volume of ca. 10 ml. Addition of ethanol (50 ml) at 0 °C produced a yellow oil which was decanted and stored in pure ethanol at 5 °C. After 24 h, a yellow hygroscopic solid was formed, filtered off under nitrogen, then washed with ethanol and dried under vacuum. Yield: 1.86 g, 45%. *Anal.* Calc. for $C_4H_{14}MoN_2O_{11}$: C, 13.26; H, 3.86; N, 7.74. Found: C, 13.18; H, 3.62; N, 7.41%.

2.3. Single-crystal X-ray diffraction

X-ray intensity data were measured with a MAR345 image plate equipped with Mo Kα graphite monochromatized radiation $\lambda = 0.71069$ Å. Data for **Ib** and **Vb** were collected at low temperature: selected crystals were mounted in inert oil and transferred quickly to the cold gas stream (100–110 K) for flashing cooling. Measurements for **II** were carried out at room temperature. Crystal data and refinement parameters are summarized in Table 1. A total of 60 images at $\Delta\phi$ of 3° and at crystal to detector distance of 120 mm were collected for **Ib**. In the case of **II**, 120 images with two different orientations of the crystal were taken at the same crystal to detector distance of 120 mm. For crystal **Vb**, 120 images with two crystal orientations were collected. After integration of the spots, the data set included 5791, 12 533, and 13 369 reflections for **Ib**, **II** and **Vb**, respectively. The three structures were solved by the Patterson methods [10], followed by difference Fourier synthesis. The structures were refined by full matrix least squares on F^2 with anisotropic thermal parameters for all the non-hydrogen atoms [11]. The H atoms were localized by Fourier difference in **Ib** (except those of two ammonium cations), not included in structure **II**, and located by Fourier difference or calculated with AFIX for **Vb**. In each structure, the H atoms were included in the refinement with a common isotropic temperature factor U of 0.034 and 0.043 Å^2 for **Ib** and **Vb**, respectively.

3. Results and discussion

3.1. Infrared spectroscopy

Table 2 lists, for compounds **I**–**VI**, the infrared bands assigned to the molybdenum-oxygen double bond, the

Table 1
Crystallographic data and structure refinement for crystals **Ib**, **II** and **Vb**

	Ib	**II**	**Vb**
Empirical formula	$C_2H_8N_2MoO_8$	$C_2H_{10}MoN_2O_9$	$C_6H_{26}Mo_2N_4O_{17}$
Formula weight	284.04	302.06	618.19
Temperature (K)	110(2)	293(2)	100(2)
Crystal system	monoclinic	orthorhombic	triclinic
Space group	$P2_1/n$	*Pnma*	$P\bar{1}$
Unit cell dimensions			
a (Å)	9.553(4)	9.148(4)	7.661(2)
b (Å)	6.391(2)	7.066(4)	11.350(5)
c (Å)	13.743(5)	14.115(6)	12.565(3)
α (°)	90	90	112.30(2)
β (°)	98.93(2)	90	101.06(2)
γ (°)	90	90	96.66(2)
V (Å^3)	828.9(5)	912.4(7)	970.4(5)
Z	4	4	2
D_{calcd} (g cm^{-3})	2.28	2.20	2.12
Absorption coefficient (mm^{-1})	1.61	1.47	1.38
$F(000)$	536	576	596
Crystal size (mm)	$0.3\times0.3\times0.2$	$0.4\times0.15\times0.15$	$0.4\times0.15\times0.15$
θ Range for data collected (°)	2.8–26.4	2.6–26.4	2.9–27.5
Index range	$0 \geqslant h \geqslant 11$	$-11 \geqslant h \geqslant 0$	$-9 \geqslant h \geqslant 9$
	$0 \geqslant k \geqslant 7$	$0 \geqslant k \geqslant 8$	$-14 \geqslant k \geqslant 14$
	$-16 \geqslant l \geqslant 15$	$0 \geqslant l \geqslant 17$	$-16 \geqslant l \geqslant 16$
Reflections collected/unique	5791/1591	12 533/993	13 369/4270
Reflections observed ($I > 2\sigma(I)$)	1545	992	3983
R_{int}	0.049	0.052	0.066
Completeness (%)	94.4	98.1	95.2
Data/restraints/parameters	1591/6/138	993/0/80	4270/80/337
R_1, wR_2 ($I > 2\sigma(I)$)	0.040, 0.118	0.042, 0.108	0.042, 0.116
Goodness-of-fit on F^2	1.353	1.413	1.072
Largest resonance peak (e Å^3)	1.20, −1.05	1.50, −1.53	1.48, −1.24

Table 2
Infrared data (cm^{-1}) for compounds **I–VI**

Compound	ν(Mo=O)	ν(O–O)	ν_{as}(COO)	ν_{s}(COO)
Ia	920m	874m	1695m	
			1686m	1400s
			1654m	
II	967s	865s	1726s	1419s
			1705s	1380s
			1684s	
III	954m	856m	1636m	1410s
IV	950m	848m	1609m	1401s
Va	956s	849s	1558s	1432s
	930m			1393s
VI	948m	856m	1624m	1400s

Note. w, weak; m, medium; s, strong.

side-bonded peroxo ligands and some representative vibrational modes of the coordinated carboxylate ligands.

In addition to the bands arising from the carboxylate ligands, each obtained spectrum shows systematically two bands of medium intensity near the values of 850 and 950 cm^{-1} correponding to the vibrational modes ν(O–O) and ν(Mo=O), respectively. Other bands due to the presence of coordinated peroxo ligands are also arising at the values of ca. 600 and ca. 650 cm^{-1} corresponding to $\nu_{as}[Mo(O_2)]$ and $\nu_{s}[Mo(O_2)]$, respectively. These bands are not listed in Table 2.

The asymmetric stretching frequency of the carboxylato groups bound to molybdenum occurs, in the spectra of the citrato, tartrato, glycolato and malato compounds, as a broad band near 1600 cm^{-1}. The coordination of the metal atom by these carboxylato groups is evidenced by the broadening of this ν_{as}(COO) band and by its shift from a value of ca. 1700 cm^{-1} in the free carboxylic acid to ca. 1600 cm^{-1} in the complex. The spectra of the oxalato compounds display three ν_{as}(COO) bands in the range 1650–1690 cm^{-1} resulting from the numerous vibrational modes of the oxalato group.

3.2. ^{13}C NMR spectroscopy

The ^{13}C NMR spectrum of the $[MoO_2(O_2)(ox)]^{2-}$ displays one single signal at the value of 167 ppm, intermediate between the single carbon signal occurring in free oxalic acid (161.4 ppm) and ammonium oxalate (173.1 ppm). This spectral shape proves that the oxalato group acts as a bidentate ligand resulting in one single carbon environment. In the ^{13}C NMR spectrum of the $[MoO(O_2)_2(ox)]^{2-}$ anion, two close lines appear at 164.8 and 167.0 ppm, revealing that complexation implies a differentiation of the two C atoms in the oxalato ligands. The ^{13}C NMR spectrum of $[MoO(O_2)_2(H_2tart)]^{2-}$is more complicated and displays two groups of resonance centered around 87 and 182 ppm, likely to arise from the hydroxyl-bearing and carboxylate carbon atoms, respectively. These carbon atoms seem to be involved in the complexation with molybdenum because they are observed in the free acid at 72.0 and 177.1 ppm. We suggest that the tartrate ligand is bidentate, with binding atoms being oxygens from one carboxylate and one hydroxyl group. Complexation should lead in that way to the formation of a five-membered chelate ring which would be consistent with the observation of Dengel et al. [4] that only carboxylate ligands which allow the formation of this type of chelate ring lead to peroxo–carboxylato complexes of Mo and W. The complexity of the resonances suggests that some decomposition of the compound in solution may have occurred. This observation is identical to that reported for the similar potassium derivative [4] which seems to decompose in a bridged tartrato complex $[Mo_2O_2(O_2)_4(tart)]^{4-}$ with the release of free tartrate in the medium. The peroxo–citrato compound probably presents a similar behavior. The ^{13}C NMR spectrum of $[MoO(O_2)_2(H_2cit)]^{2-}$ displays three groups of resonance centered around 43, 86 and 175 ppm that can be assigned to the CH_2 groups, the hydroxyl-bearing carbon and the carboxylate groups, respectively. The citrate ligand would also be bidentate, with binding oxygen atoms from the carboxylato and the hydroxyl borne by the quaternary carbon. Complexation would also in that way result in a five-membered ring. The ^{13}C NMR analysis of a solution obtained from the crystals of the peroxo-glycolato (**Vb**) compound displays resonance lines at 71.5 and 183.5 ppm occurring from the $[MoO(O_2)_2(glyc)]^{2-}$ species together with lines at 16.8 and 57.3 ppm due to the presence of co-crystallized ethanol (as will be confirmed by X-ray analysis). For comparison, resonance occurs in the free glycolic acid at 59.0 and 176.0 ppm arising from the hydroxyl-bearing CH_2 and the carboxylic groups, respectively. In the case of the $[MoO(O_2)_2(Hmal)]^{2-}$ anion, the ^{13}C NMR spectrum displays several signals at 39.4, 79.3, 179.2 and 183.5 ppm. Some additional relatively weak lines are observed, occurring from residual ethanol and probably free malic acid. The line arising at 39.4 ppm corresponds to the CH_2 group of the ligand (37.9 ppm in the free acid). Moreover, the signal corresponding to the hydroxyl-bearing CH group in the coordinated malate has undergone a significant shift from a value of 66.4 ppm in the free acid to 79.3 ppm, suggesting that this carbon is involved in Mo complexation. Finally, the two resonance signals at 179.2 and 183.5 ppm correspond to the quaternary carbons of the two carboxylate groups. In the free acid, these C atoms appear as two signals at 174.0 and 176.0 ppm. These ^{13}C NMR results suggest that the malate ligand is also bidentate, with binding atoms being oxygens from one carboxylato group and the hydroxyl group.

Table 3
Data deduced from TG analyses for compounds **I–VI**

Compound	T_F (°C)[a]	H_2O expt. (%)[b]	H_2O calcd. (%)[c]	Δm total (%)[d]	
				Expt.	Calcd.[e]
Ia	350	6.25	5.96 ($n = 1$)	50.25	52.33
II	330	0	0	54.69	52.01
III	450	0	0	62.29	64.21
IV	360	9.44	9.04 ($n = 2$)	[f]	63.83
Va	380	0	0	52.08	49.66
VI	400	4.71	4.97 ($n = 1$)	[f]	60.23

[a] Final decomposition temperature.
[b] Weight loss of the first decomposition step observed on the TG.
[c] Calculated on the basis of the molecular formula containing n water molecule(s).
[d] Total weight loss (25 °C – T_F).
[e] Weight loss calculated with respect to MoO_3.
[f] Unavailable value, explosion on heating.

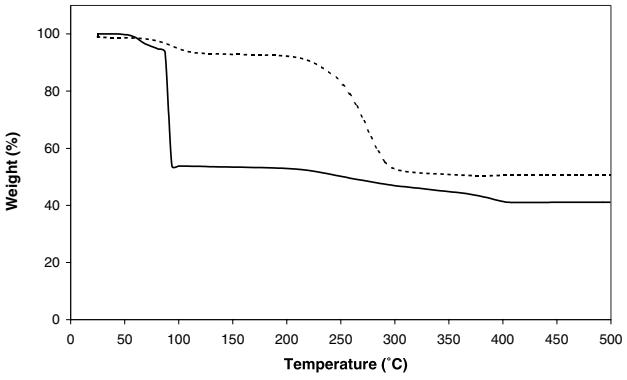

Fig. 1. Thermogravimetric analyses of compound **Ia** (dashed line) and **VI** (straight line) in air (10 °C/min).

3.3. Thermal analyses

After dehydration, the peroxo–carboxylato molybdenum(VI) complexes undergo a multi-step degradation into MoO_3 (checked by powder XRD) up to a final decomposition temperature in the range 350–400 °C. Table 3 lists, for compounds **I–VI**, the final decomposition temperature as well as the number of crystallized water molecules deduced from the TGA analyses. Because of the presence of peroxo groups, some of these compounds show a poor thermal stability. Their thermograms display a vigorous exothermal decomposition with a drastic weight loss near 100 °C. In the case of the tartrato and malato derivative, this decomposition is quite violent and leads to an explosion. The TGA of the compounds **Ia** and **VI** are illustrated in Fig. 1.

3.4. Single-crystal X-ray structure analysis

Crystallographic data for **Ib**, **II** and **Vb** are given in Table 1 and selected bond lengths and angles in Tables 4–6, respectively. The structure resolution of crystal **Ib** reveals that we obtained upon crystallization a dimeric entity, di-(μ-hydroxo)–diperoxo–dioxo–dioxalato–dimolybdate(VI). In this anion, as illustrated in Fig. 2, the

Table 4
Selected bond lengths (Å) and bond angles (°) for crystal **Ib**

Mo–O(1)	1.688(3)	Mo–Mo[a]	3.085(1)
Mo–O(2)	1.976(4)	O(2)–O(3)	1.458(4)
Mo–O(3)	1.962(3)	O(5)–C(1)	1.290(5)
Mo–O(4)[a]	1.931(3)	O(6)–C(1)	1.219(5)
Mo–O(4)	1.979(3)	O(7)–C(2)	1.264(4)
Mo–O(5)	2.126(3)	O(8)–C(2)	1.237(5)
Mo–O(7)	2.245(3)	C(1)–C(2)	1.557(6)
O(1)–Mo–O(4)[a]	102.6(1)	O(4)[a]–Mo–O(5)	151.3(1)
O(1)–Mo–O(3)	101.9(1)	O(3)–Mo–O(5)	122.1(1)
O(4)[a]–Mo–O(3)	79.7(1)	O(2)–Mo–O(5)	79.4(1)
O(1)–Mo–O(2)	97.0(1)	O(4)–Mo–O(5)	77.5(1)
O(4)[a]–Mo–O(2)	122.6(1)	O(1)–Mo–O(7)	165.4(1)
O(3)–Mo–O(2)	43.4(1)	O(4)[a]–Mo–O(7)	90.9(1)
O(1)–Mo–O(4)	98.3(1)	O(3)–Mo–O(7)	85.7(1)
O(4)–Mo–O(4)[a]	75.8(1)	O(2)–Mo–O(7)	79.9(1)
O(3)–Mo–O(4)	151.0(1)	O(4)–Mo–O(7)	79.5(1)
O(2)–Mo–O(4)	152.5(1)	O(5)–Mo–O(7)	74.0(1)
O(1)–Mo–O(5)	91.4(1)		

[a] Symmetry transformations used to generate equivalent atoms: $-x + 1, -y, -z + 1$.

two molybdenum atoms are sevenfold-coordinated and form two edge-sharing pentagonal bipyramids which are centrosymmetrical with respect to an inversion center of the unit cell. The $[Mo_2O_2(O_2)_2(\mu\text{-}OH)_2(ox)_2]^{2-}$ anion thus possesses a C_i symmetry. Both oxalato ligands are bidentate and form two five-membered chelate rings with molybdenum. In this $[Mo_2O_2(O_2)_2(\mu\text{-}OH)_2(ox)_2]^{2-}$ anion, the two terminal oxo groups (Mo–O 1.688(3) Å) and oxygen atoms from the two carboxylato groups of the oxalato ligands (Mo–O 2.126(3) Å) occupy the axial positions in both bipyramids, while oxygens from the peroxo (mean Mo–O 1.969(3), O–O 1.458(4) Å), the remaining carboxylato groups (Mo–O 2.245(3) Å) and the two slightly asymmetrically bridging hydroxo groups (Mo–O 1.979(3), Mo′–O 1.931(3) Å) constitute the equatorial plane. The molybdenum atom is displaced by 0.28 Å from the equatorial plane towards the oxo group. The axial oxygen atom O(7), *trans* to the double-bonded oxygen atom O(1), lies at a significantly longer mean distance (Mo–O 2.245(3) Å) from the molybdenum atom and is thus less tightly bound than the other oxygen atoms in the anion. This phenomenon was also observed for other seven-coordinated molybdenum(VI) peroxo complexes of the type $[MoO(O_2)_2(L)]^{2-}$ (with L = oxalate, glycolate, citrate) [4–6] and illustrates the important *trans* influence of the oxo ligand. In crystals **II**

Table 5
Selected bond lengths (Å) and bond angles (°) for crystal **II**

Mo–O(1)	1.671(3)	O(2)–O(3)	1.475(4)
Mo–O(2)[a]	1.919(3)	O(4)–C(1)	1.293(5)
Mo–O(2)	1.919(3)	O(5)–C(1)	1.208(6)
Mo–O(3)	1.955(3)	O(6)–C(2)	1.264(5)
Mo–O(3)[a]	1.955(3)	O(7)–C(2)	1.224(6)
Mo–O(4)	2.045(3)	C(1)–C(2)	1.550(5)
Mo–O(6)	2.261(3)		
O(1)–Mo–O(2)[a]	104.3(1)	O(2)[a]–Mo–O(4)	131.1(8)
O(1)–Mo–O(2)	104.3(1)	O(2)–Mo–O(4)	131.1(8)
O(2)[a]–Mo–O(2)	87.3(1)	O(3)–Mo–O(4)	88.0(8)
O(1)–Mo–O(3)	100.6(1)	O(3)[a]–Mo–O(4)	88.0(8)
O(2)[a]–Mo–O(3)	130.2(1)	O(1)–Mo–O(6)	169.3(1)
O(2)–Mo–O(3)	44.7(1)	O(2)[a]–Mo–O(6)	83.3(8)
O(1)–Mo–O(3)[a]	100.6(1)	O(2)–Mo–O(6)	83.3(8)
O(2)[a]–Mo–O(3)[a]	44.7(1)	O(3)–Mo–O(6)	79.4(1)
O(2)–Mo–O(3)[a]	130.2(1)	O(3)[a]–Mo–O(6)	79.4(1)
O(3)–Mo–O(3)[a]	157.7(2)	O(4)–Mo–O(6)	74.6(1)
O(1)–Mo–O(4)	94.7(1)		

[a] Symmetry transformations used to generate equivalent atoms : $x, -y + 3/2, z$.

Table 6
Selected bond lengths (Å) and bond angles (°) for molecule 1 of crystal **Vb**

	Anion 1	Anion 2		Anion 1	Anion 2
Mo–O(1)	1.986(2)	1.991(3)	O(1)–O(2)	1.484(3)	1.482(4)
Mo–O(2)	1.941(3)	1.940(3)	O(3)–O(4)	1.484(3)	1.484(3)
Mo–O(3)	1.952(2)	1.943(2)	O(5)–C(1)	1.272(4)	1.271(4)
Mo–O(4)	1.973(2)	1.969(3)	O(6)–C(2)	1.398(4)	1.420(4)
Mo–O(5)	2.310(2)	2.211(2)	O(8)–C(1)	1.252(4)	1.242(4)
Mo–O(6)	1.974(2)	2.011(2)	C(1)–C(2)	1.516(5)	1.516(4)
Mo–O(7)	1.680(2)	1.688(3)			
O(7)–Mo–O(2)	103.2(1)	104.5(1)	O(2)–Mo–O(1)	44.4(9)	44.3(1)
O(7)–Mo–O(3)	104.0(1)	100.7(1)	O(3)–Mo–O(1)	129.7(1)	130.4(1)
O(2)–Mo–O(3)	86.9(1)	87.4(1)	O(4)–Mo–O(1)	157.7(1)	161.4(1)
O(7)–Mo–O(4)	102.5(1)	102.4(1)	O(6)–Mo–O(1)	88.5(1)	90.3(1)
O(2)–Mo–O(4)	129.1(1)	130.7(1)	O(7)–Mo–O(5)	169.9(1)	166.6(1)
O(3)–Mo–O(4)	44.4(1)	44.5(1)	O(2)–Mo–O(5)	82.1(1)	84.6(1)
O(7)–Mo–O(6)	94.8(1)	91.5(1)	O(3)–Mo–O(5)	84.6(9)	87.1(1)
O(2)–Mo–O(6)	131.4(1)	131.9(1)	O(4)–Mo–O(5)	79.9(1)	82.6(1)
O(3)–Mo–O(6)	132.0(1)	133.5(1)	O(6)–Mo–O(5)	75.4(9)	75.5(9)
O(4)–Mo–O(6)	88.7(1)	88.3(1)	O(1)–Mo–O(5)	77.9(9)	79.1(1)
O(7)–Mo–O(1)	99.8(1)	97.9(1)			

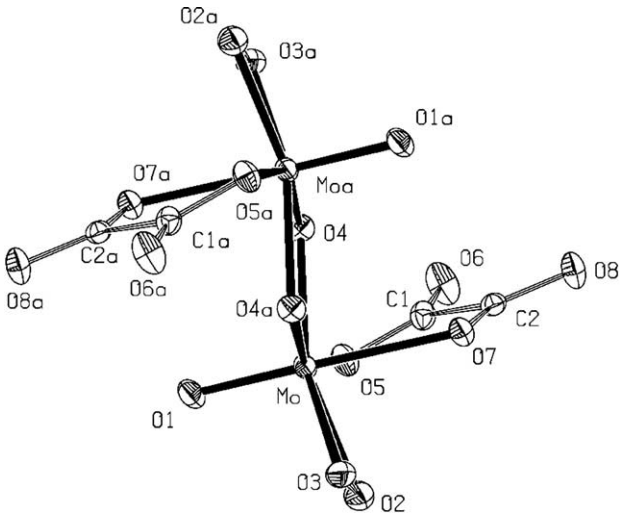

Fig. 2. ORTEP plot of the molecular anion of $[Mo_2O_2(O_2)_2(\mu\text{-}OH)_2(ox)_2]^{2-}$ (50% probability) [12].

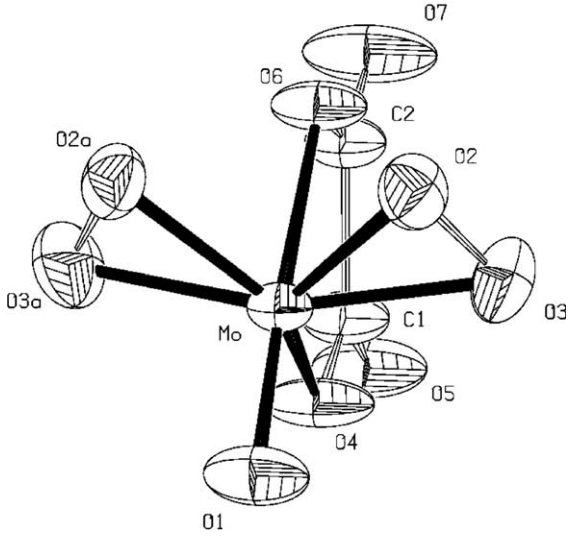

Fig. 3. ORTEP plot of the molecular anion of $[MoO(O_2)_2(ox)]^{2-}$ (50% probability) [12].

and **Vb**, as observed for the similar potassium derivatives, $K_2[MoO(O_2)_2(ox)]$ and $K_2[MoO(O_2)_2(glyc)]$ [4,5], molybdenum displays a sevenfold-coordination and it is surrounded by two side-bonded peroxo groups, one oxo and one bidentate carboxylato ligand forming a five-membered ring with molybdenum. The molecular structures of the $[MoO(O_2)_2(ox)]^{2-}$ and $[MoO(O_2)_2(glyc)]^{2-}$ anions are illustrated in Figs. 3 and 4, respectively. The coordination polyhedron is a pentagonal bipyramid, as observed in most sevenfold-coordinated transition metal diperoxo complexes. The axial positions are occupied by a terminal oxo ligand (Mo–O 1.671(3) Å for **II** and mean Mo–O 1.684(3) Å for **Vb**) and one oxygen atom from a deprotonated carboxylato group

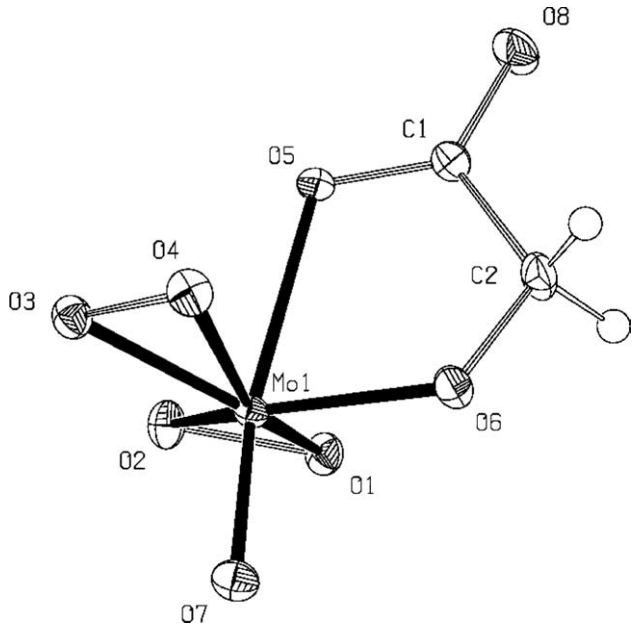

Fig. 4. ORTEP plot of the molecular anion of $[MoO(O_2)_2(glyc)]^{2-}$ (50% probability) [12].

(Mo–O 2.261(3) for **II** and mean Mo–O 2.260(3) Å for **V**). The equatorial positions are occupied by two slightly asymmetrically bound peroxo ligands (Mo–O 1.919(3) and 1.955(2) for **II**, mean Mo–O 1.944(3) and 1.979(3) Å for **V**) and an oxygen of the oxalato ligand (Mo–O 2.045(3) Å) in the case of **II** or a deprotonated hydroxyl (mean Mo–O 1.992(3) Å) in the case of **Vb**. The average value observed for O–O bond is 1.475(4) and 1.484(3) Å for **II** and **Vb**, respectively. For both **II** and **Vb**, the molybdenum atom is displaced by about 0.3 Å from the equatorial plane towards the molybdenum-oxygen double bond. The observed distances between molybdenum and oxygen atoms from peroxo, oxo, carboxylato and hydroxo groups agree well with Mo–O distances found in other peroxomolybdates [4–7].

The unit cell of crystal **II** contains two ammonium cations and one mononuclear oxo–diperoxo–oxalato–molybdate(VI) anion. Only one half of the $[MoO(O_2)_2(ox)]^{2-}$ entity is observed in the asymmetric part of the unit cell as a consequence of a mirror plane passing through the Mo atom, the oxygen atom from the oxo group and the planar oxalato ligand. All the ammonium hydrogen atoms from ammonium cations are involved in hydrogen bonds with oxygen atoms from the anion leading to a complex network. The unit cell of crystal **Vb**, illustrated in Fig. 5, consists of four ammonium cations, two crystallographically independent complex anions and one molecule of ethanol (crystallization solvent). No significant difference between the two $[MoO(O_2)_2(glyc)]^{2-}$ anions in the unit cell was observed within the experimental error. As observed for **II**, all the hydrogen atoms from the ammonium cations are

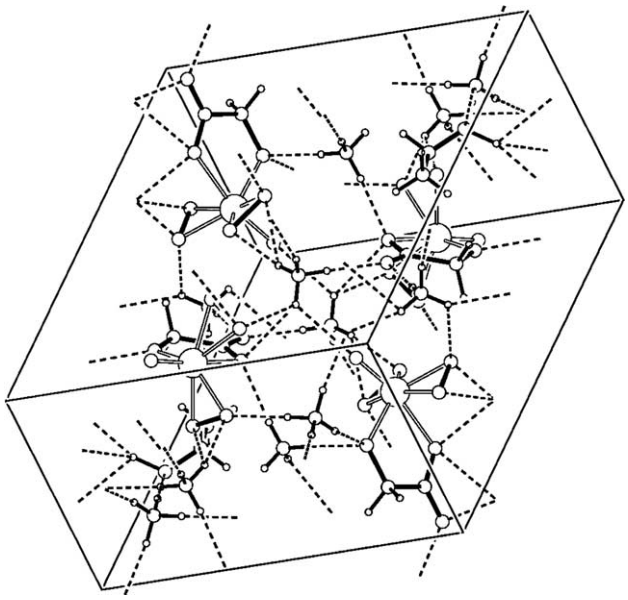

Fig. 5. Schematic view of the unit cell of **Vb** showing the hydrogen bond network.

Table 7
Hydrogen bond lengths (Å) for molecule 1 of crystal **Vb**

N100–H–O50 $(x, y, z-1)$	H–O 1.96(2); N–O 2.87(6)
N101–H–O50 $(-x, -y, 1-z)$	H–O 1.99(2); N–O 2.86(6)
O50–H–O10 $(x, y-1, z)$	H–O 1.79(2); N–O 2.80(7)

involved in hydrogen-bonds (N–O < 3 Å). Moreover, the co-crystallized ethanol molecule is hydrogen-bonded to two ammonium and to an oxygen atom from a peroxo group (Table 7).

4. Conclusions

New ammonium derivatives of peroxo molybdenum(VI) complexes with several carboxylic ligands have been prepared and characterized from the structural and spectroscopic point of view. Because these compounds exhibit a high solubility in water and contain non-metallic counter-ions, they constitute ideal candidates as precursors for Mo-based oxide materials.

5. Supplementary material

Crystallographic data for the structures in this paper have been deposited with the Cambridge Crystallographic Data Center, CCDC Nos. 212089, 212090 and 212091 for **Ib**, **II** and **Vb**, respectively. Copies of the data can be obtained, free of charge, on application to The Director, CCDC, Union Road 12, Cambridge CB2 1EZ, UK (fax: + 44-1223/336-033 or e-mail: deposit@ccdc.cam.ac.uk).

Acknowledgements

The authors thank the Belgian National Fund for Scientific Research (FNRS) for the Research fellowship allotted to D. Bayot and the financial support.

References

[1] L.C. Passoni, M.R.H. Siddiqui, A. Steiner, I.V. Kozhevnikov, J. Mol. Catal. A 153 (2000) 103.
[2] H. Mimoun, S. Patai (Eds.), The Chemistry of Peroxides, Wiley, New York, 1983.
[3] A.C. Dengel, W.P. Griffith, Polyhedron 8 (1989) 1371.
[4] A.C. Dengel, W.P. Griffith, R.D. Powell, A.C. Skapski, J. Chem. Soc., Dalton Trans. (1987) 991.
[5] R. Stomberg, Acta Chem. Scand. 24 (1970) 2024.
[6] J. Flanagan, W.P. Griffith, A.C. Skapski, R.W. Wiggins, Inorg. Chim. Acta 96 (1985) L23.
[7] A.C. Dengel, W.P. Griffith, R.D. Powell, A.C. Skapski, J. Chem. Soc., Chem. Commun. (1986) 555.
[8] A.A. Said, A.M. Al-Kority, E.M. Nour, J. Phys. Chem. Solids 53 (1992) 1245.
[9] D. Bayot, B. Tinant, M. Devillers, Catal. Today 78 (2003) 439.
[10] G.M. Sheldrick, Phase annealing in SHELX 90: Direct Methods for Larger Structures, Acta Crystallogr., Sect. A 46 (1990) 467.
[11] G.M. Sheldrick, SHELXL 93: Program for Crystal Structures Refinement, University of Göttingen, Germany, 1993.
[12] A.L. Spek, PLATON: Molecular Geometry Program, University of Utrecht, The Netherlands, 1998.